JOURNAL OF GEOPHYSICAL RESEARCH, VOL. 87, NO. C5, PAGES 3378–3384, APRIL 30, 1982

Intercomparison of Wind Speeds Inferred by the SASS, Altimeter, and SMMR

F. J. WENTZ

Remote Sensing Systems, Sausalito, California 94965

V. J. CARDONE

Oceanweather, Inc., White Plains, New York 10601

L. S. FEDOR

Wave Propagation Laboratory, NOAA, Boulder, Colorado 80303

SEASAT carried three wind speed microwave sensors: a scatterometer (SASS), an altimeter (ALT), and a five-frequency radiometer (SMMR). The winds inferred by these three sensors along with colocated in situ anemometer measurements are intercompared. The in situ comparisons show an agreement of about 2 m/s. A larger statistical data base is obtained by intercomparing the three sensors in the absence of in situ data. For nadir observations at wind speed below 10 m/s, the three instruments track each other very well and seem responsive to wind as low as 2 m/s. However, for winds above 10 m/s the ALT winds are biased low relative to the SASS and SMMR winds. The discrepancy at high wind speeds between the SASS and ALT is due to using different model functions in the geophysical processing. When properly filtered for land, sun glitter, and rain, the SASS and SMMR winds agree remarkably well. For 329 SASS and SMMR comparisons over a wind speed range from 2 to 20 m/s, the mean difference is 0.03 m/s, the standard deviation is 1.42 m/s, and the correlation is 0.95. The ability of the SMMR to measure wind speed is adversely affected by proximity to land and sun glitter. The SMMR cell must be at least 600 to 700 km from land, and the sun angle must be greater than 20° to ensure accurate winds. Both SASS and SMMR retrieve wind speeds near the eye of Hurricane Fico that are in good agreement with each other and with surface observations. Light rain of about 2 mm/h does not appear to seriously degrade the performance of the SASS or SMMR.

1. INTRODUCTION

SEASAT provides the unique opportunity to intercompare three independent on-orbit wind speed sensors. The two active sensors, the scatterometer (SASS) and altimeter (ALT), measure the microwave power that is backscattered from the sea surface. The passive microwave radiometer (SMMR) measures the radiation emitted from the sea surface and intervening atmosphere. Both the backscattered radiation and the emitted radiation are correlated with surface roughness which in turn is correlated with the wind speed near the sea surface.

The radiative backscattering is a combination of specular reflections and Bragg resonance scattering. Specular reflections occur when sea waves having wavelengths much longer than the radiation wavelength are tilted normal to the observation direction. Bragg scattering results from the incident radiation being diffracted by capillary sea waves having amplitudes small compared to the radiation wavelength. For incidence angles near nadir the specular reflections dominate, whereas at the larger incidence angles Bragg scattering is most important. In contrast, the radiometer responds to the variations in the surface emissivity caused by gravity waves tilting the sea surface and sea foam modifying the surface reflectivity. The variation of the local surface normal due to wave tilting mixes the horizontal and vertical polarized emission and changes the incidence angle for the emission. The foam acts as an impedance match for the air-water interface, thereby decreasing the reflectivity of the interface.

These physical processes that are responsible for backscattering and emission are highly correlated with the sea-surface wind speed. Wave tilting, capillary wave amplitude, and foam coverage all increase with wind speed. This correlation allows for the retrieval of wind speed from the sensor observations. There are several good references on the theory of microwave remote sensing [*Swift*, 1977; *Munn*, 1978; *Gower*, 1980].

The three SEASAT sensors have different swaths as is shown in Figure 1. The scatterometer has three separate swaths, one centered on nadir and the other two on the right and left sides. The nadir swath is ±70 km about nadir, and the off-nadir swaths begin at about 200 km cross-track from nadir and extend out to about 700 km from nadir. The altimeter swath is 2.4 to 12 km wide, depending on sea state, and is centered on nadir. The radiometer swath is 600 km wide, with one edge being about 50 km to the left of nadir and the other edge being about 550 km to the right of nadir. For the SMMR grid 1, the swath is divided into four columns 150 km wide, which is the resolution of the SMMR's lowest frequency of 6.6 GHz. For grid 2, the SMMR swath is divided into seven columns 86 km wide, which is the resolution of the SMMR's 10.7 GHz channel. The SMMR columns are numbered, starting at nadir, from 1 to 4 for grid 1 and from 1 to 7 for grid 2. Each column is divided into cells that are approximately square having a dimension of 150 km for grid 1 and 86 km for grid 2. With the exception of the four Queen Elizabeth II (QE II) revolutions discussed in section

Paper number 1C1664.
0148-0227/82/001C-1664$05.00

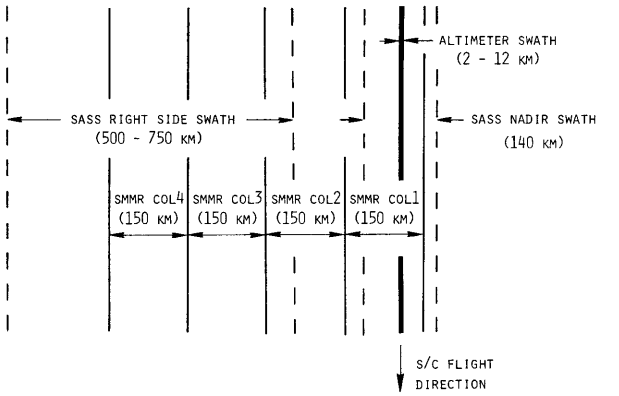

Fig. 1. Rightside swath coverage for the SASS, ALT, and SMMR.

4, the wind comparisons herein are at the grid 1 resolution. The QE II revolutions are at the grid 2 resolution. A complete description of the sensors' swath geometry and resolution capabilities is given by *Weissman* [1980].

The winds retrieved from all three sensors can be intercompared at nadir, and the SASS and SMMR winds can be compared across the SMMR swath. For the nadir comparisons, the SASS and ALT sample only the near-nadir portion of a column 1 cell, whereas the SMMR samples the entire cell. For the off-nadir comparisons on grid 1, the SASS sees only the right-half of a column 2 cell but sees all of columns 3 and 4. In the presence of strong wind gradients, these resolution differences will degrade the intercomparisons.

In section 2 we briefly describe the algorithms used to retrieve the wind speed for the three sensors and discuss how the sensors' footprints are colocated. Section 3 begins by comparing the sensor winds with in situ anemometer measurements. Then wind comparisons of the three sensors, in the absence of in situ data, are shown. The effects of proximity to land, sun glitter, and rain on the wind retrievals are discussed in section 4, and section 5 contains our conclusions. Throughout this paper we use the abbreviation 'rev.' to denote a SEASAT revolution, i.e., an orbit. When we refer to a particular rev., such as rev. 1135, we do not mean the entire orbit, but rather a segment of the orbit. In all cases we specify the extent of the orbit segment.

2. Algorithm Descriptions

The raw telemetry counts from the three sensors are processed to normalized radar cross section (NRCS) for the SASS and ALT and to brightness temperature (T_B) for the SMMR. The sensor algorithms described in the IEEE Special SEASAT Issue [*Weissman*, 1980] perform this Level 1 processing. The NRCS's and T_B's depend on the observation frequency, polarization, and viewing direction, as well as on environmental parameters. Level 2 geophysical processing is required to remove the observation dependence and obtain the environmental parameters. The geophysical processing for the SASS and SMMR is accomplished by least squares algorithms that find the environmental parameter vector **P** that minimizes the following sum of squares:

$$\mathrm{SOS} = \sum_{i=1}^{I} [M_i - F(\mathbf{P}, \mathbf{O}_i)]^2/\Delta_i^2 \qquad (1)$$

where M_i is the NRCS or T_B measurement, $F(\mathbf{P}, \mathbf{O}_i)$ is the model function corresponding to the M_i measurement, $\mathbf{O}_i$ is the observation vector for the measurement, and Δ_i^2 is the expected variance between the measurement and model function due to measurement and modeling error. The summation is over the I measurements whose footprints fall within a specified resolution cell. The ALT algorithm can be thought of as a special case of (1) where $I = 1$. The model function computes an expected value for the measurement given the environmental and observation vectors. For off-nadir observations, the SASS environmental vector consists of wind speed and wind direction. For nadir observations, the environmental vector for the SASS and the ALT has only one component, wind speed, because wind direction does not affect the nadir NRCS measurement. For the SMMR there are four components, wind speed, sea-surface temperature, atmospheric water vapor, and atmosphere liquid water. The observation vector consists of the sensor's frequency, polarization, and viewing direction. All results reported herein come from the most recent versions of the model functions. For the SASS, the SASS-I model function is used [*Schroeder et al.*, this issue]. The SMMR model function is the finalized version implemented January 30, 1981 [*Wentz*, 1981*a*]. The ALT function is described by *Fedor and Brown* [this issue].

For intercomparison purposes, we use either the grid 1 or grid 2 SMMR cell. For the grid 1 cases, the SMMR algorithm finds the least squares wind solution for the ten T_B measurements associated with the cell. For grid 2, there are only eight T_B measurements since the two polarization channels at 6.6 GHz are not included on the higher resolution grid. When processing the SASS data at the grid 1 resolution, all SASS footprints whose centroids fall within a grid 1 cell are grouped together and included in (1) to compute a single wind speed. When processing the SASS data on grid 2, pairs of orthogonal SASS measurements are first converted to a wind speed, and then the wind speeds for all pairs whose centroids fall within the grid 2 cell are averaged together. For the comparisons of the ALT winds with the in situ anemometer measurements, the ALT wind speeds come from a 6 s average of the portion of the subtrack that is closest to the anemometer. For the Gulf of Alaska revs. in which the SASS, ALT, and SMMR are intercompared, the ALT winds come from the 22 s portion of the subtrack that is within a grid 1 cell.

In developing the SMMR model function, we used SASS-inferred wind speeds for columns 3 and 4 of SEASAT revs. 1120 and 1135. These are descending revs. that go out from the Gulf of Alaska toward Hawaii. The rev. 1120 segment is 1200 km, whereas the rev. 1135 segment is much longer, extending from Gulf of Alaska to the equator. The relationship between the sea-surface emissivity and wind speed was derived from these SASS winds [*Wentz et al.*, 1981]. All other revs. reported herein were withheld from the emissivity model function development. After determining the emissivity relationships, the SMMR-inferred wind speeds for column 1 of these two revs. were used to specify the SASS model function for nadir observations. This method of model function development was chosen because of the difficulty in obtaining reliable surface-observations of winds colocated with SEASAT observations.

Although comparing SASS and SMMR winds for these two revs. is not an independent verification of performance, the agreement shown in Figure 2 between SASS and SMMR

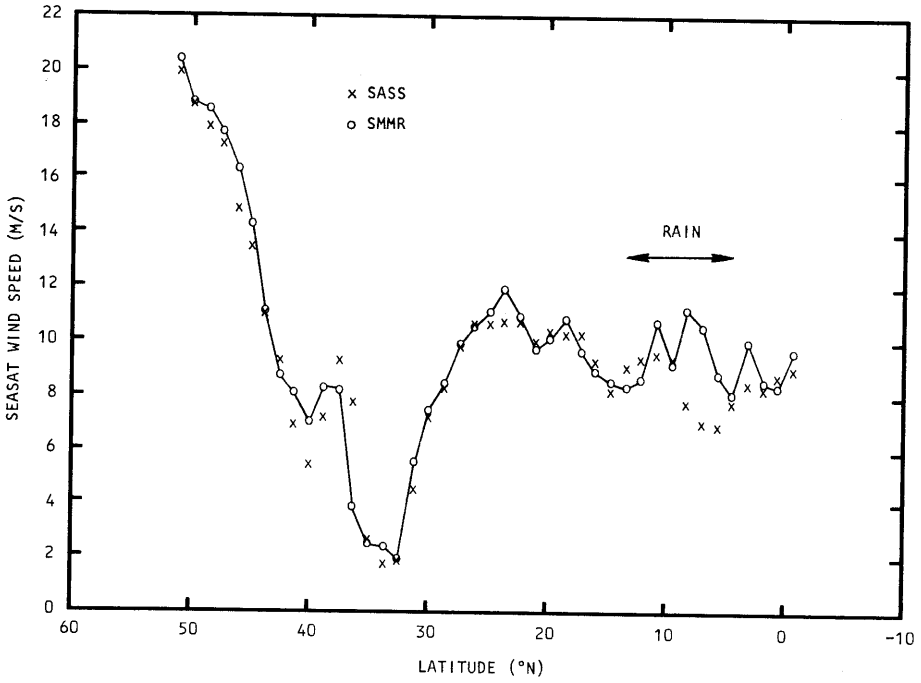

Fig. 2. A comparison of the SASS and SMMR wind speeds for grid 1, column 3 of rev. 1135.

for rev. 1135 is still quite remarkable. The correlation between SASS and SMMR winds for columns 3 and 4 of rev. 1135, excluding cells with rain, is 0.98 for 63 observations. This high correlation is due to more than simply tuning model functions. For example, consider the hypothetical case, which has been postulated in the past, of the sea-surface NRCS saturating at wind speeds above 10 m/s due to the saturation of capillary wave growth. Also assume that the wind-induced sea-surface emissivity is entirely due to foam generation that abruptly begins at 7 m/s. If this hypothesis were a true description of nature, then no amount of model function tuning could achieve the correlation of 0.98 over the wind speed range shown in Figure 2. The 3 m/s offset in the two curves near 9°N is probably due to the rain clouds in the Intertropical Convergence Zone (ITCZ), although one cannot say which sensor is being adversely affected. This rainy portion of the rev. was excluded from the emissivity derivation.

3. Wind Intercomparisons Among Remote Sensors and In Situ Anemometers

In this section we compare the winds retrieved by the three sensors with in situ anemometer measurements, and also intercompare the remotely sensed winds for a number of orbit segments for which surface data are not available. The comparisons in this section are under ideal conditions. Since all comparisons are made during the evening or at night, the SMMR data are free of any possible sea-surface sun glitter. Also we only consider cells that are at least 700 km away from land, thereby avoiding land contamination in the SMMR antenna sidelobes. Finally, if the SMMR indicates that there is rain in a cell, then that cell is excluded. The effects of land, sun glitter, and rain are discussed section 4.

To begin with, we intercompare winds from the three sensors with in situ anemometer measurements. The anemometer measurements consist of 20 from Weather Station Papa and 3 from NOAA Data Buoy 46006, both in the Gulf of Alaska. For the SASS and SMMR, the grid 1 wind speeds in the vicinity of the anemometer are interpolated to the anemometer location. For the ALT, the wind speed comes from a 6 s average of the portion of the subtrack that is closest to Papa or the buoy. The anemometer wind is reported every 6 hours and is interpolated to the time of the SEASAT overpass. Except for the one case mentioned in the next paragraph, the winds appear to be fairly constant in time. The SMMR indicated that rain was present for 5 of the 23 in situ comparisons, and these cases are excluded. Of the remaining 18 comparisons, nine are for the nadir column 1 cells. Hence these comparisons apply mostly to the nadir observation of wind speed. When this investigation was being done, not all of the SASS, ALT, and SMMR sensor data tapes were available. Also for the cases in which the anemometer is not within a column 1 cell, no ALT comparison is made. As a result the number of usable comparisons for the SASS, ALT, and SMMR is 14, 6, and 18, respectively. Although this data set is quite small, the Papa winds are very reliable.

Figure 3 is a scatter plot of SASS, ALT, and SMMR winds versus the in situ winds, and Table 1 gives the intercomparison statistics, i.e., the number of comparisons, the mean difference, and the standard deviation of the difference about the mean. The SMMR shows the best comparison with the in situ winds, having a mean difference of 0.7 m/s and a standard deviation of 1.8 m/s. The 14 SASS winds are biased 1.4 m/s high relative to the anemometer winds and show a standard deviation of 2.1 m/s. The 6 ALT winds are biased low by 1.6 m/s and have a standard deviation of 1.6 m/s. For the SASS and SMMR, the largest discrepancy with Papa, which is circled in the figure, occurs for the same rev. The SASS wind is 18.7 m/s, the SMMR wind is 17.8 m/s, and the Papa wind is only 12.6 m/s. It is interesting that the Papa report 6 hours earlier gave a 32 m/s wind. Possibly the poor agreement is due to a rapidly changing wind-sea state. When this anomalous comparison is excluded, the comparison

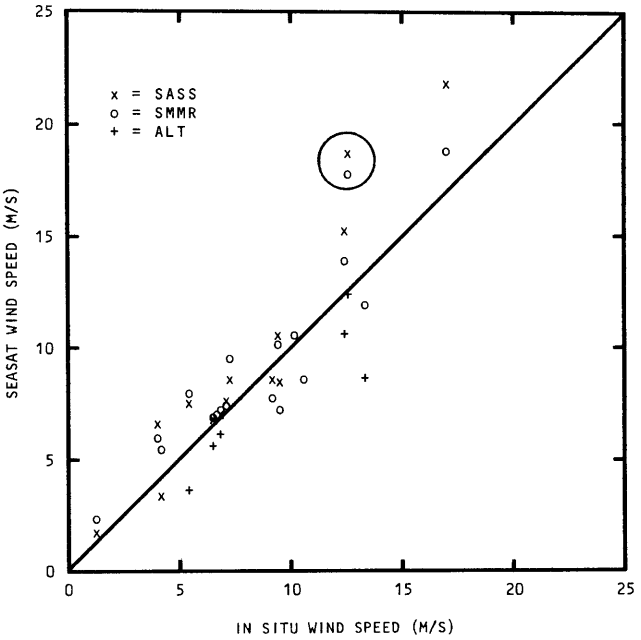

Fig. 3. SASS, ALT, and SMMR inferred wind speeds plotted versus in situ anemometer observations. The line of perfect agreement is shown.

statistics improve. The mean and standard deviation for the SMMR become 0.5 and 1.4 m/s, and for the SASS the mean and standard deviation are 1.1 and 1.7 m/s.

The best intersensor comparison is between the SMMR and SASS, showing a mean difference of −0.3 m/s and a standard deviation of 1.2 m/s. The largest intersensor discrepancy is that the ALT winds are biased low by about 3 m/s relative to the SASS and SMMR winds, particularly at winds above 10 m/s. This bias is due to the difference between the SASS and ALT model functions, as is discussed in section 5. Also there is a slight indication in Figure 3 that the SASS nadir winds may be overestimating the higher wind speeds.

The collection of reliable in situ wind data and the colocation of these data with the satellite observations are formidable tasks. While there is no substitute for good in situ winds, intercomparison of remotely sensed winds in the absence of surface data is a valuable exercise requiring considerably less resources. This is particularly true since the SASS wind-sensing performance over the primary off-nadir swath has been partially verified by the JASIN Experiment [*Jones et al.*, 1981, this issue]. Hence the SASS can be used to evaluate the SMMR wind-sensing capability. Also the response of the three sensors to various wind field features, such as high winds in storms and low winds in cols, can be compared. For instance, we can determine if the three sensors are equally responsive to low and high winds, a question that has been frequently debated.

TABLE 1. Sensor and In Situ Wind Intercomparison

Comparison Type	Number of Comparisons	Mean Differences, m/s	Standard Deviation, m/s
SASS − in situ	14	1.44	2.09
ALT − in situ	6	−1.64	1.62
SMMR − in situ	18	0.74	1.80
ALT − SASS	5	−3.33	2.31
SMMR − SASS	14	−0.30	1.21
SMMR − ALT	6	3.08	1.67

Figure 4 shows the SASS, ALT, and SMMR wind speeds plotted versus latitude for four revs. over the Gulf of Alaska: 1163, 1178, 1206, and 1221. These are descending revs. that go out from the Gulf of Alaska toward Hawaii. The lengths of these rev. segments vary from 1200 to 1800 km. The wind speeds are for the nadir column 1 cells at the 150 km grid 1 resolution. For wind speeds below 10 m/s, the three sensors track each other quite well, with each detecting an apparent low wind region near 40°N. These plots indicate that all three sensors are responsive to wind speeds as low as 2 m/s. The largest discrepancy occurs in rev. 1221 for high winds. The ALT reaches a maximum wind of 13 m/s, whereas the SMMR reaches 18 m/s and the SASS reaches 20 m/s. As mentioned above, this discrepancy between the ALT winds and the winds obtained from SASS and SMMR is due to using different model functions.

Next we compare the SASS and SMMR over the entire SMMR swath for the four Gulf of Alaska revs. mentioned above and for revs. 1120 and 1135, which were used to tune the SMMR and SASS model functions. Figure 5 is a scatter plot of SMMR winds versus SASS winds for the six revs. The solid line in the figure is the 45° line of perfect agreement. There are a total of 329 grid 1 cells, for which the mean

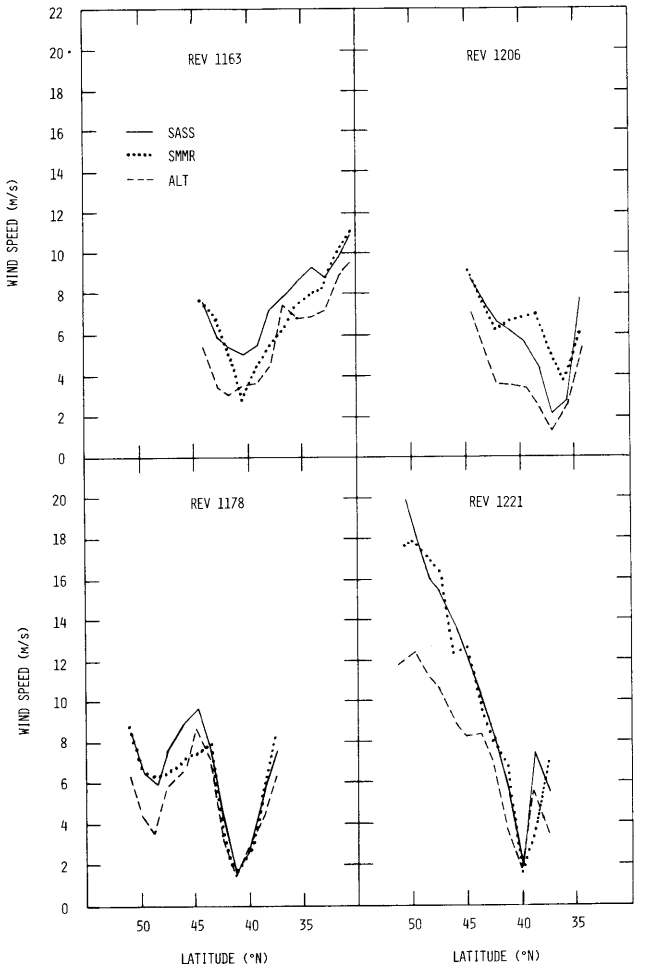

Fig. 4. Comparisons of nadir wind speeds measured by the three sensors.

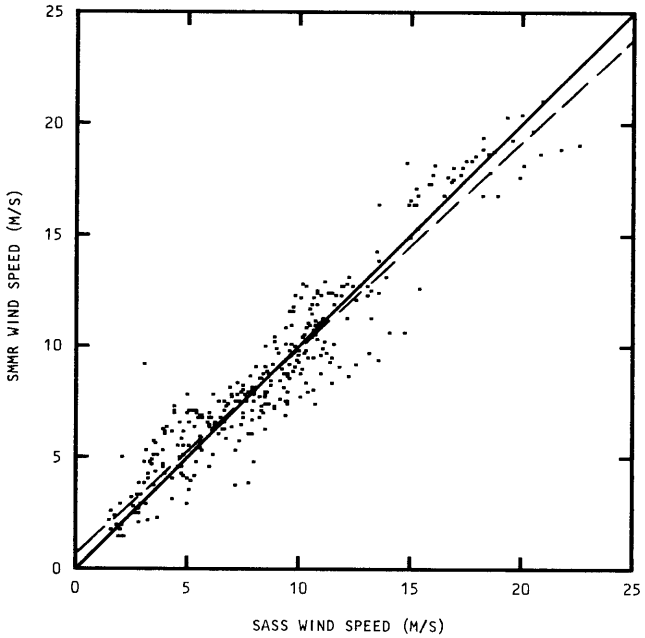

Fig. 5. A scatter plot of SMMR versus SASS winds for six North Pacific revs. Line of perfect agreement is the solid line, and the least squares fit is the dashed line.

difference of SMMR minus SASS is 0.03 m/s and the standard deviation about the mean is 1.42 m/s. The least squares fit to the 329 points, which is shown by the dashed line, has a slope of 0.925 and a y intercept of 0.7 m/s. The correlation between the two estimates of wind speed is 0.95. Table 2 gives the comparison statistics breakdown for each rev. and each column included in Figure 5. The first entry in the table is the number of samples, the second is the mean SMMR minus SASS difference, and the third is the standard deviation. The comparison statistics for revs. 1120 and 1135, which were used in model function development, are in general agreement with the statistics obtained from the four withheld revs.

TABLE 2. Wind Statistics Across the Swath

Revolution	Column Number 1	2	3	4	All Columns
1135	35*	33	33	30	131
	−0.03†	0.53	0.21	0.25	0.24
	1.48‡	1.01	0.96	1.05	1.15
1178	12	13	11	9	45
	−0.29	−0.33	−1.05	−2.00	−0.83
	0.90	2.00	2.05	1.58	1.77
1221	12	12	11	11	46
	−0.12	0.45	−0.12	−0.21	0.00
	1.59	0.78	0.83	1.37	1.18
1120	6	7	6	5	24
	−1.97	0.91	0.81	2.10	0.41
	0.82	0.99	0.90	2.26	1.92
1163	12	13	12	11	48
	−0.79	0.98	0.38	0.31	0.24
	0.95	0.88	0.90	1.27	1.17
1206	9	9	9	8	35
	0.70	−0.07	−0.97	−0.40	−0.18
	1.43	1.86	1.23	1.72	1.62
All revs.	86	87	82	74	329
	−0.24	0.43	−0.06	−0.03	0.03
	1.42	1.30	1.27	1.62	1.42

* First column entry is 'number of samples.'
† Second column entry is 'mean SMMR − SASS difference.'
‡ Third column entry is 'standard deviation.'

TABLE 3. SMMR and SASS Wind Comparisons for Revolution 1074 Near Land

Column	No. of Cells	SMMR − SASS Winds, m/s Mean	Standard Deviation
4	23	0.09	1.34
5	23	−0.64	1.36
6	18	−1.26	1.97
7	13	−2.48	2.60

4. The Effect of Land, Sun Glitter and Rain on Wind Retrieval

In this section we focus on three problems that can degrade the wind sensing performance of the three sensors. The first problem is proximity to land and primarily affects the SMMR. The second problem, sun glitter, only affects the SMMR. Third, there is rain, which in sufficient quantity can degrade the performance of all three sensors.

The effect of land and sun glitter on wind retrieval is exemplified in a series of four revs.: 1066, 1074, 1080, and 1094. The revs. are over portions of the developing North Atlantic storm which has come to be known as the QE II Storm because the luxury linear Queen Elizabeth II encountered damaging seas on September 11, 1978, in an area viewed by rev. 1094. The four rev. segments are each about 1800 km long. The rev. 1066, 1080, and 1094 segments extend from the Sargasso Sea to Newfoundland. The rev. 1074 segment goes from Nova Scotia to the Bahamas. For these revs. the SMMR and SASS winds are computed on the 86 km grid 2. Only the off-nadir columns 4, 5, 6, and 7 are considered, and hence no ALT comparisons can be made. If the SMMR indicates that rain is present in the cell under consideration or in an adjacent cell, then the cell is excluded. This careful filtering eliminates any possible data contamination due to rain.

Rev. 1074 is a nighttime, descending pass that parallels the east coast of the United States. Columns 4, 5, 6, and 7 are approximately 760, 670, 590, and 500 km from the coast. Table 3 gives the mean SMMR minus SASS wind speed difference and the standard deviation of the difference for each column. For column 4, which is farthest from land, the mean of 0.1 m/s and the standard deviation of 1.3 m/s are very similar to the values obtained in section 3 for the six Gulf of Alaska revs., which are also at nighttime and far away from land. Going from column 4 to column 7, a very large negative SMMR minus SASS wind bias develops. The bias of −2.5 m/s for column 7 is a strong indication that at 500 km from land the antenna pattern correction algorithm overcompensates for the relatively hot thermal emission of land entering the antenna sidelobes. The SASS is also affected by land, but the effect is not significant until the edge of the SASS footprint is less than 50 km from land. This is one advantage the active sensors have over the passive sensor.

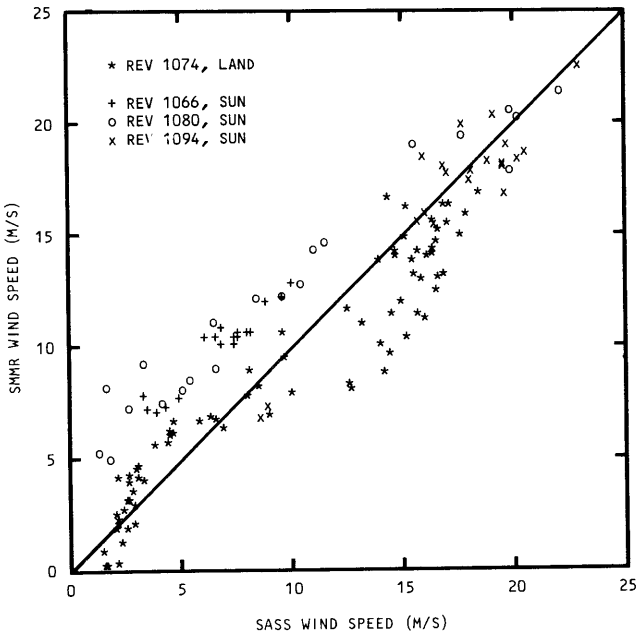

Fig. 6. A scatter plot of SMMR versus SASS winds for four North Atlantic revs. affected by land and sun glitter. The line of perfect agreement is shown.

The other three QE II revs. are during the daytime and experience sun glitter. These revs. are further out to sea than rev. 1074, and land contamination should not be a problem. A filter is applied to the data to eliminate most of the sun glitter. If the sun angle is less than 10° or if the sun angle is less than 15° and the wind speed is less than 15 m/s, then the cell is excluded. The sun angle is the angle between the vector pointing from the cell to the SMMR and the propagation vector of solar radiation that would be specularly reflected from the cell if the sea surface were flat. For sun angles less than 15°, wind speeds below 15 m/s produce more glitter directed toward the SMMR than winds above 15 m/s. For this reason, we use the two criteria sun glitter filter. Although this filtering technique eliminates a large portion of the sun glitter, there is still a residual component at sun angles out to 20° or 25°. For example, the sun glitter T_B computed from two-scale scattering theory [*Wentz,* 1978] translates into a 2, 1, and 0.3 m/s wind speed error for sun angles of 15°, 20°, and 25°, respectively, assuming that the true wind speed is 10 m/s. Hence, the SMMR winds for the three daytime revs. should be biased somewhat high because the sun glitter filter is not restrictive enough.

Figure 6 is a scatter plot of the SMMR winds versus the SASS winds for the four QE II revs. Each rev. is denoted by a different symbol. The SMMR winds from nighttime rev. 1074 are clearly biased low, most probably because of its proximity to land. In contrast, the 59 SMMR winds from the three daytime revs. are biased high about 1.9 m/s relative to the SASS because of sun glitter and the standard deviation is 2.2 m/s.

Our final wind comparison is for rev. 331 that flew over Hurricane Fico on July 20, 1978. The hurricane was southeast of Hawaii at 15.9°N and 206.6°E. The rev. segment begins in the northeast Pacific at 40°N and ends near the equator at 5°N, passing just east of Hawaii. Figure 7 shows the SASS and SMMR winds plotted versus lattiude for grid 1 column 3. In this case the rev. segment is in the evening and far away from land. However there is significant rain in the vicinity of Fico, and no rain filtering for SASS or SMMR is done. The two sensors track each other quite well. The SMMR minus SASS mean difference is 1.1 m/s and the standard deviation is 1.1 m/s for the 27 cells considered. Going north to south, both winds increase, reach a maximum at the same location, and then sharply drop. Surface wind observations indicate that the average wind speed for the two cells closest to the eye of Fico is about 20 m/s (P. Black, private communication, 1981). The SMMR retrieves a 21 m/s wind for these two cells and the SASS retrieves 20 m/s. There is no apparent degradation due to the rain bands in Fico.

There are several reasons why the rain is not seriously degrading the sensors' performance. First, at a resolution of 150 km the small rain bands tend to be washed out. The SMMR-inferred rain rate for the two cells closest to Fico is only about 2 mm/h. Also, for grid 1 retrievals the SMMR relies heavily on the 6.6 GHz channel, which is least affected by rain. Finally, the atmospheric model function for the SMMR least squares algorithm and the SASS attenuation correction algorithm uses Mie absorption coefficients to account for radiative scattering from rain drops [*Wentz,* 1981*a*,*b*]. However, we are not saying that the degradation due to light rain is entirely negligible. Referring back to Figure 2, we see a 3 m/s offset between the SASS and SMMR winds near 9°N. This offset is probably due to rain clouds in the ITCZ. Averaged over 150 km, the SMMR measured the ITCZ rain rates to be about 2 mm/h. We cannot make any definite conclusion as to which sensor is being adversely

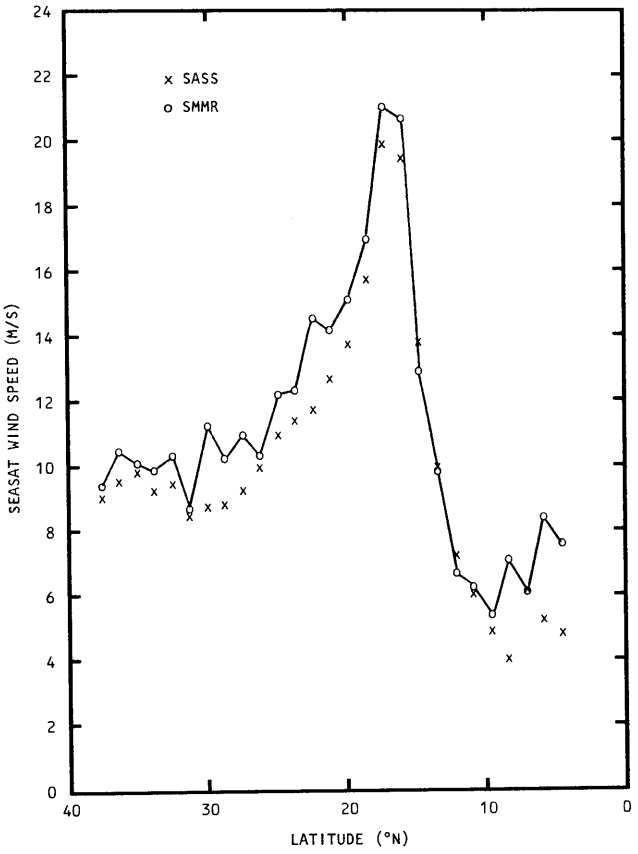

Fig. 7. A comparison of SASS and SMMR wind speeds for Hurricane Fico for grid 1, column 3 of rev. 331.

affected by the rain in the ITCZ. However, it is interesting that the SMMR winds go up a little in the ITCZ while the SASS winds go down. This behavior is exactly what happens when the atmospheric attenuation is underestimated. The SMMR brightness temperatures increase with increasing attenuation, and hence an underestimation of attenuation is compensated by an overestimation in wind speed. In contrast, the SASS NRCS decreases with attenuation, and underestimating the attenuation causes the retrieved wind speeds to be too low. If this is the case, then the light rain is causing a +1.5 m/s bias in SMMR winds and a −1.5 m/s bias in the SASS winds, which is not a substantial error.

5. CONCLUSIONS

For a limited number of in situ comparisons under favorable conditions, the SASS, ALT, and SMMR winds agree with anemometer measurements to within about 2 m/s. The data base for evaluating the three sensors is then expanded by intercomparing the winds from the three sensors in the absence of in situ data. For wind speeds below 10 m/s, the three sensors track each other very well and seem responsive to wind speeds as low as 2 m/s. However, for wind speeds above 10 m/s, the ALT winds are biased low relative to the SASS and SMMR winds. The model functions used for the SASS and ALT are markedly different for winds above 10 m/s. For example, given the same sea-surface nadir NRCS of 10 dB, the SASS model function predicts a wind speed of 17 m/s and the ALT model function predicts a 10 m/s wind. This difference in models can explain the observed difference between ALT and SASS winds; however, we do not have enough in situ observations at the higher winds to determine which sensor is more correct. To further add to the mystery, *Schroeder et al.*, [this issue] reports that the SASS nadir winds are indeed indeed accurate, while *Fedor and Brown* [this issue] indicate that the ALT is retrieving unbiased winds.

When properly filtered for rain, land, and sun glitter, the SASS and SMMR winds are in very close agreement. A total of 329 comparisons show a mean of 0.03 m/s and a standard deviation of 1.42 m/s. The correlation for these comparisons is a 0.95. The winds from the two sensors track one another from wind speeds as low as 2 m/s up to wind speeds as high as 20 m/s. Neither instrument shows any apparent lack of sensitivity over the 2 to 20 m/s range.

The ability of the SMMR to measure wind speed is adversely affected by proximity of land and sun glitter. It appears that the SMMR cell must be at least 600 to 700 km from land to obtain accurate wind speeds. Also sun glitter from the sea-surface significantly biases the SMMR winds for sun angles up to 20°. However, accurate winds could probably be obtained in the presence of sun glitter by means of a fairly simple algorithm that uses the known sun angle.

When a 150 km resolution cell is used, the performance degradation due to light rain in the cell does not appear to be too serious. Both the SASS and SMMR retrieve wind speeds near the eye of Hurricane Fico that are in good agreement with surface observations.

The major shortcoming of our analysis is that there are so few data. We have looked at only a fraction of the SEASAT Mission. By expanding the three-sensor wind data base to the entire mission, the capability of measuring winds from space can be fully assessed and understood.

Acknowledgments. We would like to acknowledge all the members of the SEASAT Intercomparison Panel who assisted in this research. W. L. Grantham and E. M. Bracalente of NASA Langley and G. S. Brown of Applied Science Associates, Inc., contributed to the wind and NRCS nadir comparisons between SASS and ALT. C. T. Swift of NASA Langley was responsible for some of the first wind intercomparisons between SASS and SMMR. E. P. McClain of NOAA/NESS and G. G. Dome of the University of Kansas provided a comparison of the atmospheric attenuation inferred by the SMMR and that inferred by the Visible and Infrared Radiometer. R. C. Beal of the Applied Physics Laboratory and F. I. Gonzalez of NOAA/PMEL did an analysis of the SASS winds versus the Synthetic Aperture Radar relative NRCS. In addition, J. W. Sherman and P. M. Woiceshyn made valuable contributions to the intercomparison analysis. This research was cosponsored by NASA Langley Research Center under contract NAS1-16032 and the SEASAT Data Utilization Project at the Jet Propulsion Laboratory under NASA contract NAS7-100.

REFERENCES

Fedor, L. S., and G. S. Brown, Wave height and wind speed measurements from the SEASAT radar altimeter *J. Geophys. Res.*, this issue.

Gower, J. F. S. (Ed.), *Passive Radiometry of the Ocean*, D. Reidel, Hingham, Mass., 1980.

Jones, W. L., F. J. Wentz, and L. C. Schroeder, Microwave scatterometer measurements of oceanic wind vector, in *Oceanography From Space*, Plenum, New York, 1981.

Jones, W. L., et al., The SEASAT-A satellite scatterometer: The geophysical evaluation of remotely sensed wind vector, *J. Geophys. Res.*, this issue.

Munn, R. E. (Ed.), Special issue on radio oceanography, *Boundary Layer Meteorol., 13*, 1–429, 1978.

Schroeder, L. C., The relationship between wind vector and normalized radar cross section used to derive SEASAT-A satellite scatterometer winds, *J. Geophys., Res.*, this issue.

Swift, C. T. (Ed.), Special joint issue on radio oceanography, *IEEE J. Oceanic Eng., OE-2*(1), 1–159, 1977.

Weissman, D. E. (Ed.), Special issue on SEASAT-1 sensors, *IEEE J. Oceanic Eng., OE-5*(2), 71–182, 1980.

Wentz, F. J., The forward scattering of microwave solar radiation from a water surface, *Radio Sci., 13*(1), 131–138, 1978.

Wentz, F. J., Model function for ocean microwave brightness temperatures, RSS Tech. Rep., Remote Sensing Systems, Sausalito, Calif., Aug. 1981*a*.

Wentz, F. J., The effect of atmospheric attenuation on microwave scatterometer measurements, RSS Tech. Rep., Remote Sensing Systems, Sausalito, Calif., Sept. 1981 *b*.

Wentz, F. J., E. J. Christensen, and K. A. Richardson, Dependence of sea-surface microwave emissivity on friction velocity as derived from SMMR/SASS, in *Oceanography From Space*, Plenum, New York, 1981.

(Received December 16, 1980;
revised October 22, 1981;
accepted October 26, 1981.)